第35卷 第1期 焊 接 学 报 Vol. 35 No. 1
2014年1月 TRANSACTIONS OF THE CHINA WELDING INSTITUTION January 2014

基于贝叶斯图像模式识别技术的点焊质量评估

张宏杰[1,2]， 张建业[1,2]， 隋修武[1,2]
(1. 天津工业大学 机械工程学院，天津 300387; 2. 天津工业大学 天津市现代机电装备重点实验室，天津 300387)

摘 要: 提出一种将点焊过程动态电极位移信号转化为二值图像的方法. 基于图像特征分析，从焊点样本电极位移二值图像中提取出15个隐含特征. 针对一系列对应不同焊接质量焊点样本电极位移二值图像特征，利用主成分分析消除图像特征间的互相关性，建立了基于最小风险贝叶斯图像识别技术的焊点质量分类器. 分类器有效性测试结果表明，电极位移信号二值图像尽可能多的保留了焊点质量信息，特征提取算法简单、高效、易于实现; 同时在小数据样本情况下，贝叶斯图像识别技术能够快速、准确地评判焊点质量，有较好的应用前景.

关键词: 电阻点焊; 质量评估; 贝叶斯统计分析; 图像识别
中图分类号: TG409 **文献标识码**: A **文章编号**: 0253-360X(2014)01-0109-04

0 序 言

点焊过程动态信号蕴含大量直接或间接反映焊点质量的信息[1-4]. 随着现代信号分析与数据挖掘技术的发展，基于点焊过程动态信号特征分析进行焊点质量评估受到广泛关注[5-8]. 目前，点焊质量无损评估主要通过点焊过程动态电阻、电极力、电极位移等信号的时、频域特征分析，提取监测特征参量，利用神经网络、回归分析等方法建立监测特征与焊点质量评价指标间的非线性映射模型或分类器，进而实现焊点质量评判. 但此类方法通常建立在大量数据样本基础上，监测特征的获取与焊点质量的评判涉及复杂的数据处理与算法，影响了其在实际生产中的应用，因此在小数据样本情况下，寻找监测特征获取简单、焊点质量评估快速准确、适合实际生产的方法是非常必要的.

文中以点焊过程电极位移为监测信号，提出一种将位移信号转化为二值图像的方法，同时利用主成分分析实现图像特征的提取，并基于贝叶斯图像识别技术实现小样本情况下的焊点质量评判.

1 电极位移信号及二值图像

试验信号采集系统由恒流方式控制的交流电阻点焊机、传感器、信号调理及采集单元构成，针对0.7 mm板厚的低碳钢板进行搭接点焊. 电极力2 kN，电极头工作面直径6 mm，焊接电流3.2～4.4 kA，共获取焊点样本50个. 图1为电极位移信号波形及二值图像. 图1a为焊接电流4.4 kA，焊接时间0.4 s，信号时长0.5 s时的电极位移波形，图1中a点对应断电时刻.

传统基于动态信号特征分析进行点焊质量评估的方法只关注采样数据与质量评价指标间的映射关系，忽略了信号本身的图像信息. 实际上不同焊点质量对应不同的电极位移波形图像，因此对焊接质量的识别即是对波形图像特征的识别. 获取位移波形图像可以通过网格划分方法实现. 图1b为图1a中电极位移波形网格划分结果，纵轴通过将前述50个焊点样本电极位移幅值范围15等分实现. 将波形曲线穿过的网格区域用黑色方块代替即可得到位移波形二值图像，如图1c所示，但这种方法算法设计复杂，因此文中提出了一种新颖的图像获取方法. 在位移波形网格化处理之后，求取每个焊点样本电极位移信号的周波位移均值，并查找各周波位移均值在纵轴15段位移区间中所属的位置，图1d所示为查找区间后得到的二值图像，其中黑色区域对应周波位移均值在15段区间中的位置; 将图1d中的黑色、白色方块分别用1、0代替，可以得到表征位移二值图像的二值化矩阵.

2 贝叶斯图形识别技术

贝叶斯图像识别技术采用错误率或风险值作为判别函数或决策依据. 当样本总数为 N，样本类别总数为 M，抽样前各类别 w_i，$i=1,2,\cdots,M$ 中包含 N_i 个样本时，定义先验概率 $P(w_i)$ 为

收稿日期: 2012-09-25

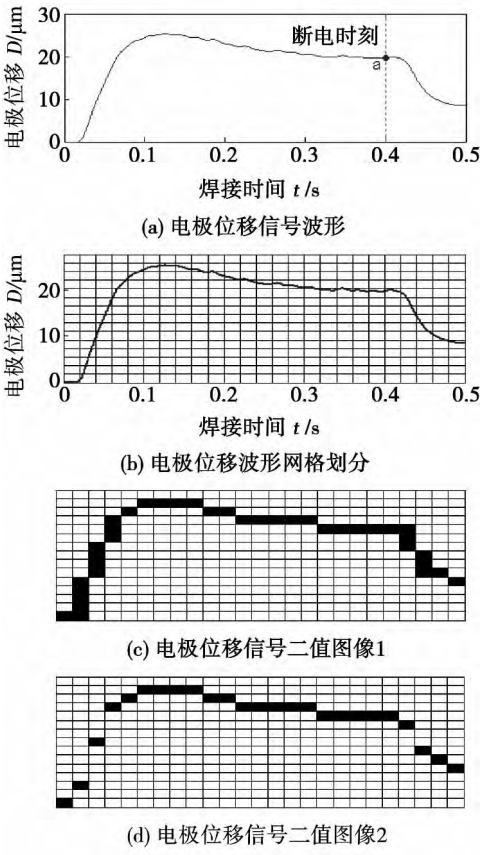

图 1 电极位移信号波形及二值图像

Fig. 1 Electrode displacement curve and its binary image

$$P(w_i) = N_i/N \tag{1}$$

多数情况下，类条件概率密度函数 $P(X|w_i)$ 可以采用多维变量的正态密度函数模拟，即

$$P(X|w_i) = -\frac{1}{2}(\boldsymbol{X}-\boldsymbol{X}^{(w_i)})^{\mathrm{T}} S_i^{-1}(\boldsymbol{X}-\boldsymbol{X}^{(w_i)}) - \frac{n}{2}\ln 2\pi - \frac{1}{2}\ln|S_i| \tag{2}$$

式中：X 为样本特征向量；$\boldsymbol{X}^{(w_i)}$ 为 w_i 类的均值向量；S_i 为 n 维协方差矩阵，定义为

$$S_i = \frac{1}{N_i - 1}\sum_{j=1}^{N_i}(\boldsymbol{X}_j - \boldsymbol{X}^{(w_i)})(\boldsymbol{X}_j - \boldsymbol{X}^{(w_i)})^T \tag{3}$$

式中：X_j 为 w_i 类中第 J 个样本特征向量.

这样对于待测样本，贝叶斯公式可以算出该样本分属于各类别的后验概率为

$$P(w_i|X) = \frac{P(X|w_i)P(w_i)}{\sum_{j=1}^{M}P(X|w_j)P(w_j)} \tag{4}$$

图像识别中，错误的识别是难以避免的，如何给出正确的判决是贝叶斯决策所讨论的问题. 目前最具代表性的贝叶斯决策包括基于最小错误率判别或基于最小风险判别决策. 对于焊接质量评估工作，基于最小风险的判别决策更为适合.

若待测样本具有属性 X，其实际类别为 w_i，后验概率为 $P(w_i|X)$，定义损失函数为 $\lambda(\alpha_k, w_i)$，表示待测样本本身属于 w_i，而决策 α_k 将其归属为类别 w_k 造成的损失，若决策 α_i 的条件风险 $R(\alpha_i|X)$ 为

$$R(\alpha_i|X) = \sum_{j=1}^{M}\lambda(\alpha_i, w_j)P(w_i|X),\ i = 1,2,\cdots,M \tag{5}$$

其中，损失函数为

$$\lambda(\alpha_i, w_j) = \begin{cases} 0 & i = j \\ 1 & i \neq j \end{cases} \quad i,j = 1,2,\cdots,M \tag{6}$$

则最小风险贝叶斯决策规则为

$$R(\alpha_j|X) = \min_{i=1,2,\cdots,M} R(\alpha_i|X) \tag{7}$$

3 位移图像特征提取与识别算法设计

特征提取与选择是图像模式识别的关键. 图 2 为前述 50 个焊点样本在每种焊接电流参数下任意选出的 3 个位移信号二值图像. 观察发现，不同电流参数下电极位移二值图像差异明显，因此依据电流参数的类别将位移二值图像分为 5 类. 二值图像每列中黑色区域的位置表征了点焊过程不同时刻电极位移累计值.

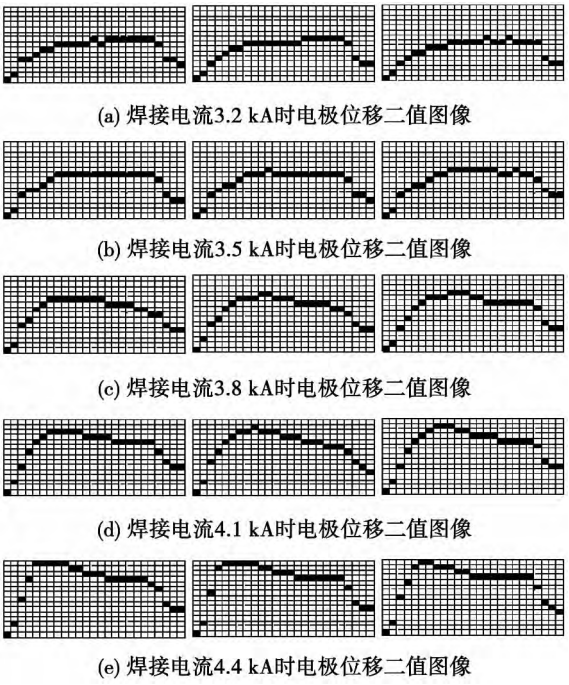

图 2 不同焊接电流参数下电极位移二值图象

Fig. 2 Binary images of electrode displacement from different welding current specifications

与文字识别常用方法类似，对二值图像采用按行求白色区域面积分数的方法提取图像特征，这样

每个焊点样本对应一 15 × 1 特征向量，图 3 给出了二值图像特征提取示意图.

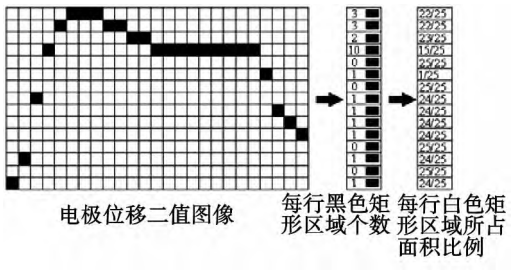

图 3　位移二值图像特征提取示意图

Fig. 3　Schematic diagram for feature extraction of displacement binary image

试验采用交叉有效性检验方法测试焊点质量分类器的有效性，过程如下：首先依次取出每个数据样本作为测试样本，对样本库中剩余焊点样本的电极位移图像特征进行主成分分析(principal component analysis，PCA) ，依据累计贡献率大于 95% 的原则选取主成分特征；利用所得主成分构建新的特征空间，并基于最小风险贝叶斯分类决策进行焊点质量判别，直到所有焊点样本都作为测试样本进行了分类器检验.

4　焊点质量分类结果

试验选取焊点接头剪切力作为质量评价指标，图 4 给出了 50 个焊点样本实测剪切力的分布情况，接头剪切力大于 2.89 kN(对应图 4 中虚线) 时，认为焊点质量合格，否则不合格，即当焊点样本被划分至类别 3，4，5 时，焊点质量合格；焊点被归属于 1，2 类时，焊点质量不合格.

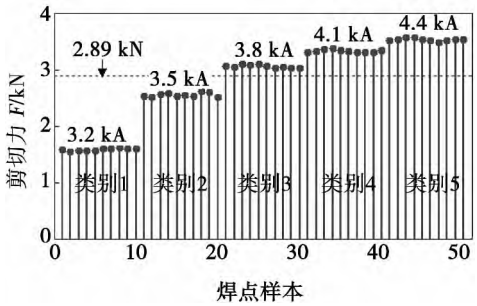

图 4　焊点接头剪切力分布

Fig. 4　Tensile shear strength of classified welded spots

图 5 为焊点质量分类器交叉有效性检验结果. 符号“o”和“* ”分别代表焊点的实际类别和识别类别. 观察发现只有焊接电流 4.4 kA 时的第七个样本出现了错分，其实际类别为 5，被识别为第 4 类. 表 1 给出了该样本作为测试样本时其余样本主成分分析结果，这里只列出了前 7 个较大特征根，其中前 5 个特征根的累计贡献率为 95.9%，对应的特征向量用来计算主成分特征.

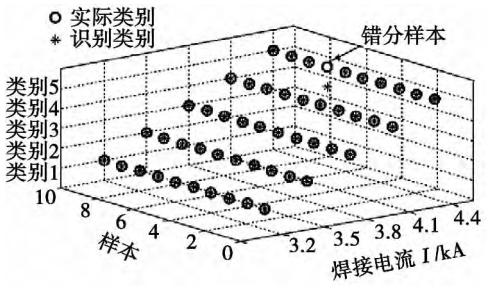

图 5　PCA-Bayesian 方法的焊点质量评估结果

Fig. 5　Quality recognition results of welds based on PCA-Bayesian method

表 1　主成分分析结果

Table 1　Results of PCA analysis

特征值序号	特征值 λ_i	贡献率 θ(%)	累计贡献率 α(%)
1	0.046 3	47.27	47.27
2	0.023 0	23.49	71.76
3	0.015 6	15.91	86.67
4	0.006 6	6.77	93.44
5	0.002 4	2.46	95.90
6	0.001 1	1.12	97.02
7	0.000 9	0.94	97.96

图 6 为错分焊点样本所属类别样本剪切力分布情况，其中 B 点对应错分焊点样本，其实测剪切力为 3.473 kN，在同类样本中强度最低，图 6b 给出了错分样本的位移二值图像，与图 6a 中 A，C 点对应样本的二值图像相比差异明显. 贝叶斯判别分类器风险值计算结果如表 2 所示，样本属于类别 5 的风险

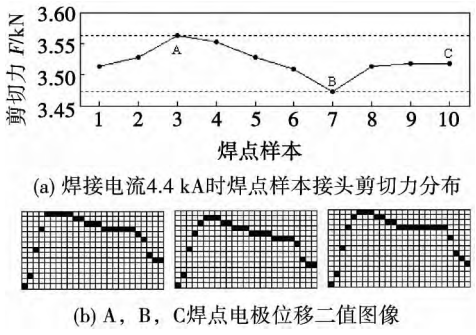

(a) 焊接电流4.4 kA时焊点样本接头剪切力分布

(b) A，B，C焊点电极位移二值图像

图 6　错分焊点样本强度及二值图像

Fig. 6　Strength and binary image of wrong classified weld

值为 -1.1709×10^4 大于属于类别 4 的风险值 -1.1720×10^4，表明其模式特征更接近第 4 类焊点样本. 从质量评估的角度，此类错分可以忽略.

表 2 贝叶斯判别风险值结果

Table 2 Risk value results of PCA-Bayesian method

焊点类别	类别 1	类别 2	类别 3	类别 4	类别 5
风险值 $\sigma(10^4)$	−0.796 8	−0.500 0	−1.047 8	−1.172 0	−1.170 9

5 异常焊接过程焊点质量评判

实际点焊过程焊点质量受多种因素影响，如焊接过程存在分流现象、焊件表面油污、焊点靠近焊件边缘等都会影响焊接区电流密度，进而影响焊点质量，为了检验分类器对不良焊点的识别能力，试验选取来自分流焊接、表面油污、近边缘焊接等异常焊接过程的 6 个焊点样本对分类器进行了检验.

表 3 给出了焊点样本质量判别结果. 由于异常焊接条件造成焊接区电流密度降低，实测焊点剪切力较相同焊接电流参数下正常焊接过程的焊点明显降低，特别是焊接电流 3.8 kA 时，异常焊接过程导致焊点质量不合格，但分类器能够根据焊点样本电极位移二值图像特征对焊点质量进行准确评判.

表 3 异常焊接过程焊点质量识别结果

Table 3 Quality recognition results of welds from abnormal welding processes

测试样本	焊接电流 I/kA	焊点来源	剪切力 F/kN	归属类别
1	4.1	分流	3.133	3
2	3.8	分流	2.732	2
3	4.4	近边缘	3.387	4
4	3.8	近边缘	2.879	2
5	4.1	表面油污	3.117	3
6	3.8	表面油污	2.836	2

6 结 论

(1) 所提出的利用点焊过程电极位移二值图像特征进行质量评估的方法是可行的. 位移二值图像尽可能多的保留了焊点质量信息，图像特征获取简单、高效、易于实现.

(2) 小样本情况下，将主成分分析和贝叶斯图像识别技术相结合能够快速、准确地实现焊点质量评判，特别对于分流焊接、表面油污、近边缘焊接等异常焊接过程焊点质量也能够准确评估.

参考文献:

[1] Hao M, Osman K A. Development in characterization of the resistance spot welding of aluminum [J]. Welding Journal, 1996, 75(1): 1s-8s.

[2] Cho Y, Rhee S. Primary circuit dynamic resistance spot monitoring and its application to the quality estimation during resistance spot welding [J]. Welding Journal, 2002, 81(6): 104s-111s.

[3] 潘存海，杜素梅，宋永伦. 铝合金点焊位移信号时频域分析与质量判定 [J]. 焊接学报，2007，28(7)：32-35.
Pan Cunhai, Du Sumei, Song Yonglun. Displacement signal time-frequency domain analysis and quality judgment of aluminum alloy resistance spot welding [J]. Transactions of the China Welding Institution, 2007, 28(7): 32-35.

[4] Wang X F, Li Y B, Meng G X. Monitoring of resistance spot weld quality using electrode vibration signals [J]. Measurement Science and Technology, 2011, 22(4): 1-11.

[5] 张宏杰，侯妍妍. 基于核 Fisher 判别分析的点焊质量评估 [J]. 焊接学报，2011，32(6)：105-108.
Zhang Hongjie, Hou Yanyan. Quality estimation of resis-tance spot welding based on kernel fisher discriminant analysis [J]. Transactions of the China Welding Institution, 2011, 32(6): 105-108.

[6] Mart'n O, López M, Mart'n F. Artificial neural networks for quality control by ultrasonic testing in resistance spot welding [J]. Journal of Materials Processing Technology, 2006, 183(3): 226-233.

[7] Podržaj P, Polajnar I. Expulsion detection system for resonance spot welding based on a neural network [J]. Measurement Science and Technology, 2004, 15(2): 592-598.

[8] Jou M. Real time monitoring weld quality of resistance spot welding for the fabrication of sheet metal assemblies [J]. Journal of Materials Processing Technology, 2004, 132(1): 102-113.

作者简介：张宏杰，男，1977 年出生，博士，讲师. 主要从事智能焊接技术与应用的研究工作. 发表论文 15 篇. Email: zhanghj022@163.com

neering, South China University of Technology, Guangzhou 510641, China). pp 95 – 100

Abstract: The effect of nano-Sb addition on the growth kinetics of intermetallic compound (IMC) in the joints with Sn-3.0Ag-0.5Cu-xSb (x = 0, 0.2, 1.0, and 2.0%) solder in reflow process was investigated. Scanning electron microscope (SEM) was used to observe the microstructure evolution of soldered joints, energy dispersive X-ray (EDX) and x-ray diffractometer (XRD) were used to identify the IMC phases. The results show that some nano-Sb particles were dissolved in Sn-rich phase, some participated in the formation of Ag_3Sb, and the rest dissolved in Cu_6Sn_5 IMC layer. The thickness of IMC layer decreased when the nano-Sb was added. Under the isochronal conditions, the thickness of IMC layer in all soldered joints was minimum when the amount of nano-Sb increased to about 1.0%. The growth exponent n and diffusion coefficient D for IMC layer were determined by curve-fitting. The results reveal that the growth exponent n and diffusion coefficient D decreased with the increase of nano-Sb content. When the amount of nano-Sb increased to about 1.0%, the growth exponent n and diffusion coefficient D were 0.326 and 10.31×10^{-10} cm^2/s, respectively. Based on the phase diagram analysis and adsorption theory, Sb had better affinity to Sn, and it could reduce the activity of Sn by forming SnSb compound, resulting in decreased driving force and surface energy for formation of Cu-Sn IMC. Therefore, the growth rate of Cu_6Sn_5 grains was suppressed and the growth of IMC layer was retarded.

Key words: reflow soldering; nano-Sb dopant; lead free solder; intermetallic compound

Gas transfer flux activating TIG welding process for aluminum alloy HUANG Yong[1,2], LI Tao[2], WANG Yanlei[2] (1. State Key Laboratory of Gansu Advanced Non-ferrous Metal Materials, Lanzhou University of Technology, Lanzhou 730050, China; 2. Key Laboratory of Non-ferrous Metal Alloys, The Ministry of Education, Lanzhou University of Technology, Lanzhou 730050, China). pp 101 – 104

Abstract: A new activating TIG welding process, gas transfer flux activating TIG (GTFA-TIG) welding, is proposed for welding aluminum alloy by changing the introduction method of active elements. In this process, a flux is transferred to shielding gas through an automatic powder feeder, and the shielding gas carries the active elements into the welding arc and weld pool. In this way, the welding arc is contracted, and the flow pattern in the weld pool is changed, finally, the weld depth increases. Without coating the flux, the automation of welding process is realized. Compared to the conventional AC TIG welding, the effects of fluxes on the weld shape, tensile property and defects of GTFA-TIG welding with eight kinds of single-component fluxes were investigated. It proves that most of halide and oxide fluxes can improve the weld depth up to 2.5-3.0 times of that of traditional TIG welding, while the effect of Te flux is less effective. The tensile strength of the joint with V_2O_5 flux is close to that of base metal, but it is lower than that of base metal when using $MnCl_2$ and AlF_3 fluxes. The X-ray detection of defects shows that the welds with V_2O_5, $MnCl_2$ and AlF_3 fluxes are assessed as grade I, while that with Te flux is grade III.

Key words: GTFA-TIG welding; aluminum alloy; arc contraction; activating flux

Microstructure and mechanical properties of welded joint of nanostructured bainite steel with regeneration FANG Kun[1], HUANG Nan[2], YANG Jianguo[1,3], SONG Kuijing[1], FANG Hongyuan[1] (1. State Key Laboratory of Advanced Welding and Joining, Harbin Institute of Technology, Harbin 150001, China; 2. Armor Force Technique Institute of PLA Teaching and Training Department, Changchun 130117, China; 3. Institute of Process Equipment and Control Engineering, Zhejiang University of Technology, Hangzhou 310032, China). pp 105 – 108

Abstract: Due to the poor weldability of nanostructured bainite steel, a method called welding with regeneration was proposed to obtain a welded joint with the same microstructure as the base metal, so the welded joint could possess the excellent mechanical properties. Regeneration treatment was used after tungsten inert gas (TIG) welding of nanostructured bainite steel. The microstructures of the welded joint were characterized by X-ray diffraction, scanning electron and transmission electron microscopes. The tensile and microhardness tests were carried out to evaluate the mechanical properties. The results show that nanostructured bainite was obtained in the fusion zone and quenched zone with 300 nm and 70 nm thick bainite plates, respectively. The tensile strength of the welded joint was 1 500 MPa, and the microhardness in the fusion zone was 7 000 MPa, which were almost equivalent to those of the base metal.

Key words: nanostructured bainite steel; regeneration; welding; nano-scale plate; strength

Quality assessment for resistance spot welding based on Bayesian image recognition technology ZHANG Hongjie[1,2], ZHANG Jianye[1,2], SUI Xiuwu[1,2] (1. School of Mechanical Engineering, Tianjin Polytechnic University, Tianjin 300387, China; 2. Tianjin Key Laboratory of Modern Mechatronics Equipment Technology, Tianjin Polytechnic University, Tianjin 300387, China). pp 109 – 112

Abstract: A method for converting electrode displacement signal to binary image in resistance spot welding process is proposed. Based on image characteristic analysis, fifteen image features are extracted from the binary image of electrode displacement waveform. The principal component analysis is used to remove the cross correlation among image features, and a series of weld specimens with different welding quality are selected to develop a quality classifier. The test results based on Bayesian image recognition technology of minimum risk show that it is feasible and reliable to utilize the binary image of electrode displacement signal to evaluate the weld quality and the image conserves the information of the weld quality. The algorithm for image feature extraction is simple, efficient and easy to use. At the mean time, the Bayesian image recognition technique with small samples can realize the welding quality assessment rapidly and accurately, and the method has a broad application prospect.

Key words: resistance spot welding; quality assessment; Bayesian statistic analysis; image recognition